Journal of the Brazilian Society of Mechanical Sciences and Engineering (2019) 41:439
https://doi.org/10.1007/s40430-019-1950-1

TECHNICAL PAPER

Importance of entropy generation and infinite shear rate viscosity for non-Newtonian nanofluid

F. Sultan[1] · W. A. Khan[2,3] · M. Ali[1] · M. Shahzad[1] · H. Sun[2] · M. Irfan[4]

Received: 2 February 2019 / Accepted: 12 September 2019 / Published online: 20 September 2019

Abstract
This study addresses the novel characteristics of infinite shear rate viscosity and entropy generation in magneto-mixed convective flow of cross-nanomaterial toward a stretched surface. Moreover, analysis of current research work has been prepared for Brownian moment and thermophoresis deposition. Radiation and viscous dissipation aspects are accounted. More specifically, roles of activation energy and Lorentz force on nanofluids transportation are examined. ODEs are acquired from PDEs via implementation of suitable transformations. Numerical algorithm is implemented to tackle the nonlinear system for numerical results. Discussion on rheological parameters involved in current research work is presented through graphs. Results demonstrate the significant rise in temperature and nanoparticles concentration with the intensification of Brownian moment aspects. More specially, we perceived that entropy rate is significantly affected by radiation parameter and Brinkman number. Intensification in entropy rate is observed for rising values of magnetic parameter, radiation parameter and Brinkman number.

Keywords Cross-fluid · Entropy generation · Magnetohydrodynamic (MHD) · Activation energy · Mixed convection

List of symbols

u, v	Velocity components
x, y	Space coordinates
ρ	Density of fluid
ν	Kinematic viscosity
μ	Dynamic viscosity
n	Power law index
B_0	Uniform magnetic field strength
$(\rho c)_{\mathrm{f}}$	Heat capacity of fluid
T	Ratio of heat capacity
$(\rho c)_p$	Effective heat capacity
α	Thermal diffusivity
σ^{**}	Stefan–Boltzmann constant
D_{T}	Thermophoresis effect
k_f	Thermal conductivity
c_p	Specific heat capacity
m^*	Mean absorption coefficient
D_{B}	Brownian motion
T	Temperature
T_∞	Ambient temperature
C_∞	Ambient concentration
T_w	Surface temperature
C_w	Surface concentration
k_{r}^2	Reaction rate
E_{a}	Activation energy
Γ	Time material constant
β^*	Ratio of viscosities
C	Concentration
m	Fitted rate constant
c	Dimensional constant
U_w	Stretching velocity
η	Dimensionless variable
We	Weissenberg number
Pr	Prandtl number

Technical Editor: Cezar Negrao, PhD.

✉ F. Sultan
faisal_maths@hu.edu.pk

✉ W. A. Khan
waqar_qau85@yahoo.com; waqarazeem@bit.edu.cn

1 Department of Mathematics and Statistics, Hazara University, Mansehra 21300, Pakistan

2 School of Mathematics and Statistics, Beijing Institute of Technology, Beijing 100081, China

3 Department of Mathematics, Mohi-ud-Din Islamic University, 12010 Nerian Sharif, Azad Jammu and Kashmir, Pakistan

4 Department of Mathematics, Quaid-I-Azam University, Islamabad 44000, Pakistan

M	Magnetic parameter
Nr	Buoyancy ratio parameter
λ	Mixed convection parameter
R	Thermal radiation parameter
Nb	Brownian motion parameter
Nt	Thermophoresis parameter
Ec	Eckert number
Sc	Schmidt number
σ	Dimensionless reaction rate
E	Dimensionless activation energy
δ	Temperature difference parameter
τ_w	Wall shear stress
q_w	Wall heat flux
f	Dimensionless velocities
θ	Dimensionless temperature
ϕ	Dimensionless concentration
N_G	Entropy generation rate
α_2	Dimensionless temperature ratio variable
α_1	Dimensionless concentration ratio variable
L	Diffusive variable
Br	Brinkman number
C_{fx}	Skin fraction
Nu_x	Local Nusselt number
Re_x	Local Reynolds number

1 Introduction

In today's world, the ever-increasing consumption of energy demands preservation in its transportation and utilization. More specifically, nanotechnology is proved to be the best mean of heat transportation and preservation among the thermal sources. Thermo-physical properties of working liquid have a great impact on the efficiency of thermal systems. Nanofluids (NFs) are obtained by mixing solid nanoparticles (NPs) in the base liquids (BLs) which have considerably greater thermo-physical properties as compared with base liquids (BLs). The achieved NFs have distinct chemical and physical features than traditional BLs. Furthermore, NFs have vital role in the improvement of cooling rate with superior thermal efficiency. Khan and Khan [1] considered rheological properties of NPs for Oldroyd-B fluid with heat sink-source. Sheikholeslam et al. [2] studied the aspects of NPs for CuO–water NFs with Lorentz forces. Khan and Khan [3, 4] reported characteristics of non-Newtonian fluid in the presence of NPs. Waqas et al. [5] deliberated characteristics of non-Newtonian fluid with appliance of NPs. Khan et al. [6] analytically analyzed properties of 3D Burgers nanofluid (NF) by considering revised heat flux relation. Khan and Khan [7] investigated appliance of NPs for Burgers NFs in the presence of heat sink-source. Hayat et al. [8] analyzed Lorentz forces and porosity aspects to investigate appliance of NFs for exponentially stretched surface. Ahmad et al. [9] numerically analyzed features time-dependent Sisko NF. Khan et al. [10] described gyrotactic microorganisms for Burgers NF with appliance of NPs. Waqas et al. [11] numerically conveyed characteristics of Williamson fluid accounting Brownian moment and thermophoresis aspects. Khan et al. [12] scrutinized radiation and Lorentz force aspects on 3D Carreau NF utilizing zero flux relation at stretched surface. Waqas et al. [13] reported properties of heat sink-source and stratified flow for Oldroyd-B NF. Sohail et al. [14] considered properties of convectively heated surface for time-dependent second grade NF in the presence of Lorentz force and zero mass flux relation. Khan et al. [15] analytically investigated properties of NPs for generalized Burgers fluid with chemical phenomenon. Animasaun et al. [16] reported the appliance of thermoelectric and Lorentz force for CuO–water NF. Recent analysis on NFs subjected to distinct flow aspects is reported in Refs. [17–42].

The bonding between the chemical components is loosening by catalysis. The catalytic reactions occur in both homogeneous/heterogeneous reactions. In homogeneous catalytic reaction system, both the catalytic materials lie in the same phase space like (gas, liquid or solid). However, in the heterogeneous process, the catalytic material lies in different phase space. Nowadays, there are wide applications of catalysts in industrial processes. More common examples that are in the agricultural and industrial process are fog formation, production of polymer, etc., when we need to start a binary chemical process, we require the minimum amount of energy, i.e., activation energy. The binary chemical process is a reaction process that occurs in two steps. Basically, the binary chemical reactions are common in both vapor and liquid deposition process. The mass transportation with chemical reaction and activation energy has industrial applications such as an oil reservoir, chemical engineering, oil emulsion, coating of metallic objects and glasses, manufacturing of electronic devices. Khan et al. [43, 44] reported properties of chemical process for non-Newtonian fluids. Mahanthesh et al. [45] considered aspects of Lorentz's force and chemical processes for NF utilizing vertical plate. Characteristics of chemical processes and modified heat flux relation were deliberated by Sohail et al. [46]. Hayat et al. [47] described features of Lorentz's force and chemical reactive species for third grade fluid. Irfan et al. [48] considered characteristics of variable conductivity and heat sink-source for non-Newtonian fluid with chemical processes. Khan et al. [49] characterized entropy generation and activation energy (AE) aspects for NF. Khan et al. [50] reported properties of AE and radiation for 3D flow of cross-NF with chemical processes. Waqas et al. [51] numerically analyzed properties of Darcy–Forchheimer and activation energy for NF in cylindrical surface. Khan et al. [52] reported appliance of chemical processes and radiative flow for cross-fluid.

Main objective of the present attempt is to examine aspects of infinite shear rate viscosity and entropy generation for magneto-mixed convective flow of cross-nanomaterial toward a stretched surface. Colloidal analysis for cross-fluid is scrutinized by considering Buongiorno relation. Transportation of heat-mass analysis is studied by utilizing activation energy and Brownian moment aspects. More specifically, aspects of viscous dissipation are considered here. System of PDE's is transformed to one and then solved by implementing MATLAB tool bvp4c. Important physical quantities are discussed through tables and graphs.

2 Problem structure

Here, characteristics of infinite hear rate viscosity and entropy optimization rate in mixed convective flow of cross-nanofluid are analyzed. Viscous dissipation activation energy aspects effects are accounted in mathematical formulation. More specifically, colloidal analysis of cross-nanofluid is permeated through Lorentz's force aspects. Characteristics of thermophoresis and Brownian movement are accounted here. Governing equations for considered flow are

$$\frac{\partial u}{\partial x}+\frac{\partial v}{\partial y}=0, \tag{1}$$

$$\begin{aligned} u\frac{\partial u}{\partial x}+v\frac{\partial u}{\partial y} =&\upsilon\frac{\partial^2 u}{\partial y^2}\left[\beta^*+(1-\beta^*)\frac{1}{1+(\Gamma\frac{\partial u}{\partial y})^n}\right]+\upsilon(1-\beta^*)\frac{\partial u}{\partial y}\frac{\partial}{\partial y}\left[\frac{1}{1+(\Gamma\frac{\partial u}{\partial y})^n}\right]\\ &-\frac{\sigma^* B_0^2}{\rho_f}u+g\left[A_1\left(T-T_\infty\right)+A_2\left(C-C_\infty\right)\right], \end{aligned} \tag{2}$$

$$\begin{aligned} u\frac{\partial T}{\partial x}+v\frac{\partial T}{\partial y} =&\frac{v}{c_p}\left(\frac{\partial u}{\partial y}\right)^2\left[\beta^*+(1-\beta^*)\frac{1}{1+(\Gamma\frac{\partial u}{\partial y})^n}\right]+\alpha\frac{\partial^2 T}{\partial y^2}+\tau\frac{D_{\mathrm{T}}}{T_\infty}\left(\frac{\partial T}{\partial y}\right)^2\\ &+\tau D_{\mathrm{B}}\frac{\partial C}{\partial y}\frac{\partial T}{\partial y}-\frac{1}{(\rho c)_f}\frac{16\sigma^{**}T_\infty^3}{3k^*}\frac{\partial^2 T}{\partial y^2}, \end{aligned} \tag{3}$$

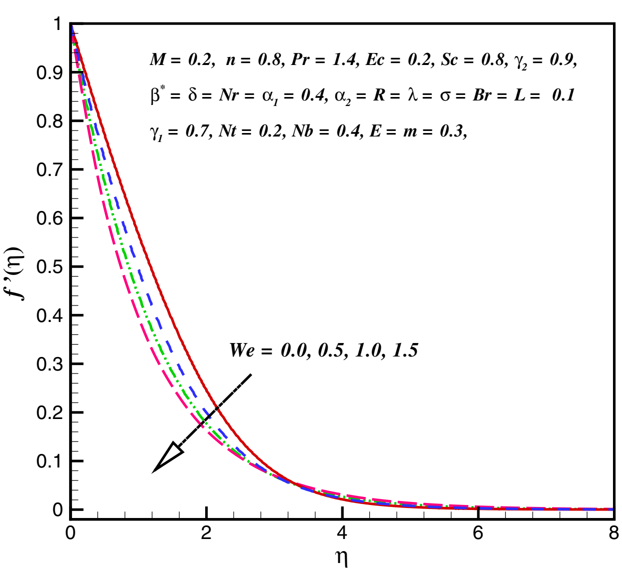

Fig. 1 $f'(\eta)$ via We

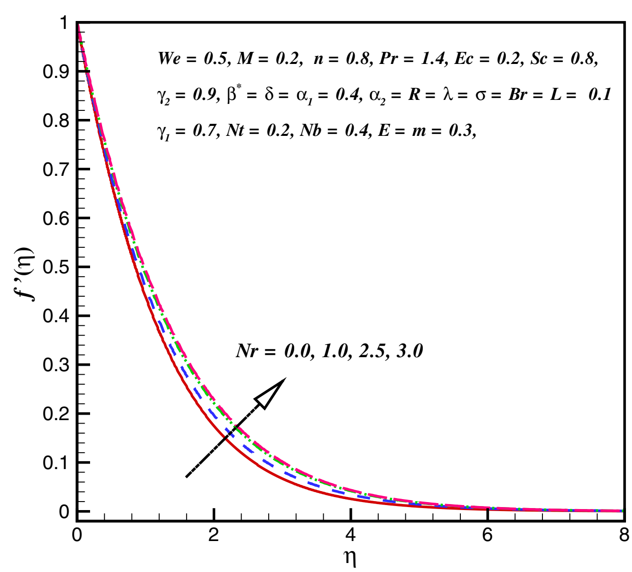

Fig. 2 $f'(\eta)$ via Nr

$$u\frac{\partial C}{\partial x}+v\frac{\partial C}{\partial y}=\frac{D_{\mathrm{T}}}{T_\infty}\frac{\partial^2 T}{\partial y^2}+D_{\mathrm{B}}\frac{\partial^2 C}{\partial y^2} - k_{\mathrm{r}}^2\left(C-C_\infty\right)\left(\frac{T}{T_\infty}\right)^m \exp\left(-\frac{E_{\mathrm{a}}}{\kappa T}\right), \tag{4}$$

with constraints

$$u=U_w=cx,\quad v=0,-k\frac{\partial T}{\partial y}=h_f(T_f-T), \quad D_{\mathrm{B}}\frac{\partial C}{\partial y}=h_\phi(C-C_\phi)\quad \text{at } y=0, \tag{5}$$

$$u\to 0,\quad T\to T_\infty,\quad C\to C_\infty\quad \text{as } y\to\infty. \tag{6}$$

Considering the following transformations

$$\eta=y\sqrt{\frac{c}{\nu}},\quad v=-\sqrt{c\nu}f(\eta),\quad u=cxf'(\eta) \quad \theta(\eta)=\frac{T-T_\infty}{T_f-T_\infty},\quad \phi(\eta)=\frac{C-C_\infty}{C_\phi-C_\infty}. \tag{7}$$

Conservation law of mass is verified identically, and remaining flow expressions become

$$\left[\beta^*\left\{1+\left(Wef''\right)^n\right\}^2+(1-\beta^*)\left\{1+(1-n)\left(Wef''\right)^n\right\}\right]f''' - \left[1+\left(Wef''\right)^n\right]^2\left[f'^2+ff''+\lambda(\theta+Nr\phi)\right]=0, \tag{8}$$

$$\left(1+\frac{4}{3}R\right)\theta''+Pr\left[f\theta'+Nb\theta'\phi'+Nt\theta'^2 +Ecf''^2\beta^*+(1-\beta^*)\frac{Ecf''^2}{1+(Wef'')^n}\right]=0, \tag{9}$$

$$\phi''+Sc\left[f\phi'+\frac{Nt}{Nb}\theta''-\sigma(1+\delta\theta)^m\phi\exp\left(-\frac{E}{1+\delta\theta}\right)\right]=0, \tag{10}$$

$$f(0)=0,\quad f'(0)-1=0,\quad f'(\infty)\to 0, \tag{11}$$

$$(0)=-\gamma_1[1-\theta(0)],\quad \theta(\infty)\to 0, \tag{12}$$

$$\phi'(0)=-\gamma_2[1-\phi(0)]\quad \phi(\infty)\to 0. \tag{13}$$

Non-dimensional form of variables occurring in Eqs. (8)–(13) is given below

$$\begin{gathered}
M=\frac{\sigma^* B_0^2}{\rho_f c},\quad Nr=\frac{gA_2\left(C_w-C_\infty\right)}{gA_1\left(T_w-T_\infty\right)}=\frac{Gr_x^*}{Gr_x},\quad \lambda=\frac{gA_1\left(T_w-T_\infty\right)}{c^2 x}=\frac{G_{rx}}{Re_x^2},\\
Pr=\frac{\nu}{\alpha},\quad R=\frac{4\sigma^{**}T_\infty^3}{k_f m^*},\quad Nb=\frac{\tau D_B\left(C_w-C_\infty\right)}{\upsilon},\quad Nt=\frac{\tau D_{\mathrm{T}}\left(T_w-T_\infty\right)}{\nu T_\infty},\quad \sigma=\frac{kr^2}{c},\\
Ec=\frac{c^2x^2}{c_p\left(T_w-T_\infty\right)},\quad We=\frac{\Gamma cx}{\nu},\quad Sc=\frac{\nu}{D_B},\quad E=\frac{E_{\mathrm{a}}}{\kappa T_\infty},\quad \delta=\frac{T_w-T_\infty}{T_\infty},\quad \beta^*=\frac{\mu_\infty}{\mu_0}.
\end{gathered} \tag{14}$$

3 Quantities of physical interest

In this section, we express surface drag force $\left(C_{fx}\right)$ and heat/mass transfer rates $\left(Nu_x, Sh_x\right)$ in dimensional forms

$$C_{fx}=\frac{\tau_{\mathrm{w}}}{\rho U_w^2}, \tag{15}$$

$$Nu_x=\frac{xq_{\mathrm{w}}}{k\left(T_w-T_\infty\right)}, \tag{16}$$

$$Sh_x=\frac{xj_w}{D_{\mathrm{B}}\left(C_w-C_\infty\right)}, \tag{17}$$

where

$$\tau_{\mathrm{w}}=\mu\frac{\partial u}{\partial y}\left[\beta^*+(1-\beta^*)\frac{1}{1+\left(\Gamma\frac{\partial u}{\partial y}\right)^n}\right], \tag{18}$$

$$q_{\mathrm{w}}=-k\frac{\partial T}{\partial y}, J_{\mathrm{w}}=-D_{\mathrm{B}}\frac{\partial C}{\partial y}. \tag{19}$$

From Eq. (15) to (17), one obtains

$$C_{fx}Re_x^{1/2}=\left[\beta^*+(1-\beta^*)\frac{1}{1+(Wef''(0))^n}\right]f''(0), \tag{20}$$

$$Nu_x Re_x^{-1/2}=-\left[1+\frac{4}{3}R\right]\theta'(0), Sh_x Re_x^{-1/2}=-\phi'(0). \tag{21}$$

Where $Re_x=\frac{xU_w}{\nu}$.

4 Entropy generation

Here, dimensional form of entropy generation is expressed as

$$S_G = \frac{k_f}{T_\infty^2}\left[1+\frac{16\sigma^* T_\infty^3}{3k_f k^*}\right]\left(\frac{\partial T}{\partial y}\right)^2 + \frac{\mu}{T_\infty}\left(\frac{\partial u}{\partial y}\right)^2\left[\beta^* + (1-\beta^*)\frac{1}{1+\left(\Gamma\frac{\partial u}{\partial y}\right)^n}\right] + \frac{\sigma^* B_0^2 u^2}{T_\infty} + \frac{R_D}{C_\infty}\left(\frac{\partial C}{\partial y}\right)^2 + \frac{R_D}{T_\infty}\left(\frac{\partial T}{\partial y}\frac{\partial C}{\partial y}\right). \tag{22}$$

In dimensionless, one has

$$N_G = \alpha_1\left[1+\frac{4}{3}R\right]\theta'^2 + Br\left[\beta^* + \frac{(1-\beta^*)}{1+(Wef'')^n}\right]f''^2 + MBrf'^2 + \frac{\alpha_2}{\alpha_1}L\phi'^2 + L\theta'\phi', \tag{23}$$

where

$$Br = \frac{\mu U_w^2}{\kappa\,\Delta T},\quad \alpha_1 = \frac{\Delta C}{C_\infty},\quad \alpha_2 = \frac{\Delta T}{T_\infty},\quad N_G = \frac{\nu T_\infty S_G}{\kappa c\,\Delta T},\quad L = \frac{R_D(C_w - C)}{k_f}. \tag{24}$$

Mathematically, Be is defined as

$$Be = \frac{\text{Entropy generation subject to heat and mass transfer}}{\text{Total entropy generation}}, \tag{25}$$

$$Be = \frac{\alpha_1\theta'^2 + + \frac{\alpha_2}{\alpha_1}L\phi'^2 + L\theta'\phi'}{\alpha_1\theta'^2 + Br\left[\beta^* + \frac{1-\beta^*}{1+(Wef'')^n}\right]f''^2 + MBrf'^2 + \frac{\alpha_2}{\alpha_1}L\phi'^2 + L\theta'\phi'}. \tag{26}$$

5 Graphical consequences and physical argument

Here, our objective is to analyze the consequences of sundry non-dimensional variables on velocity, temperature, concentration, surface drag force, entropy optimization rate, Bejan

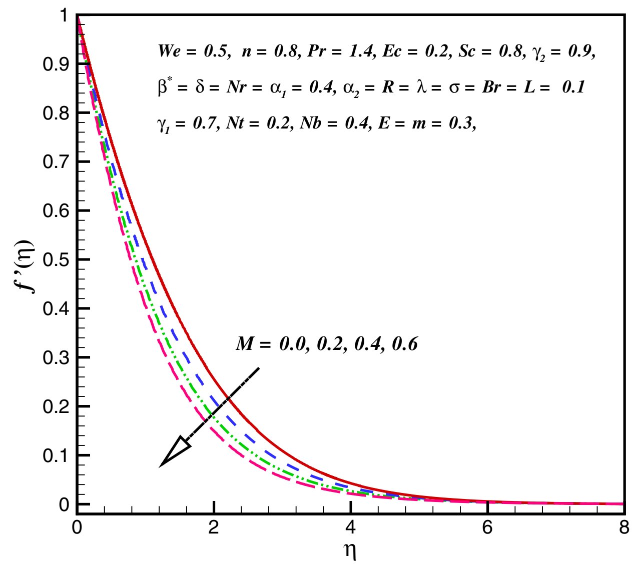

Fig. 4 $f'(\eta)$ via M

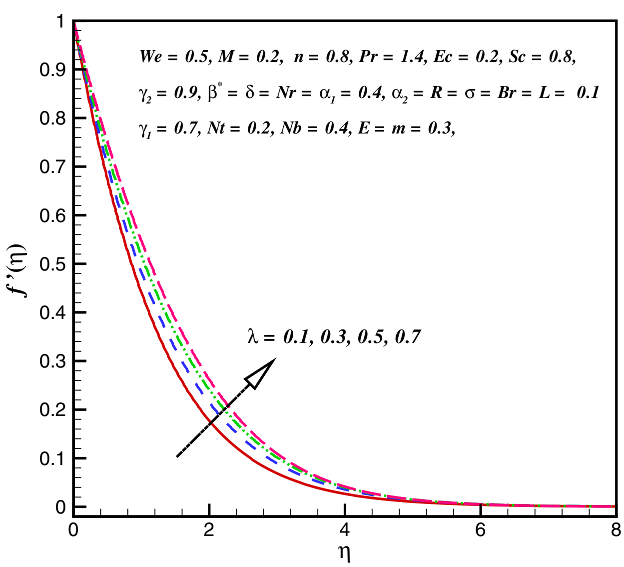

Fig. 3 $f'(\eta)$ via λ

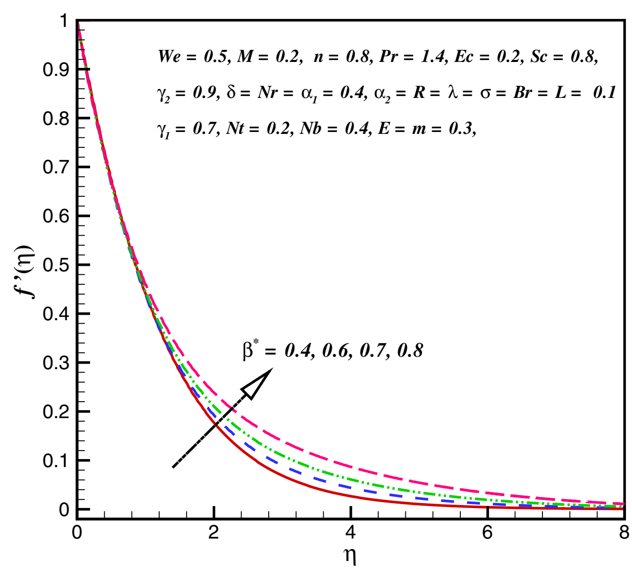

Fig. 5 $f'(\eta)$ via β^*

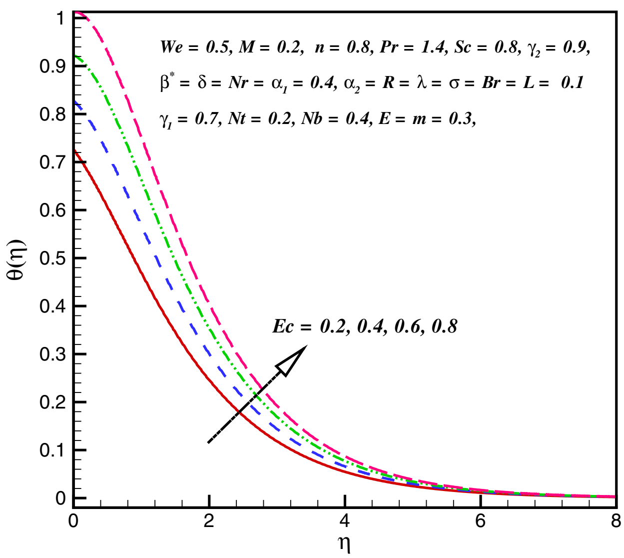

Fig. 6 $\theta(\eta)$ via Ec

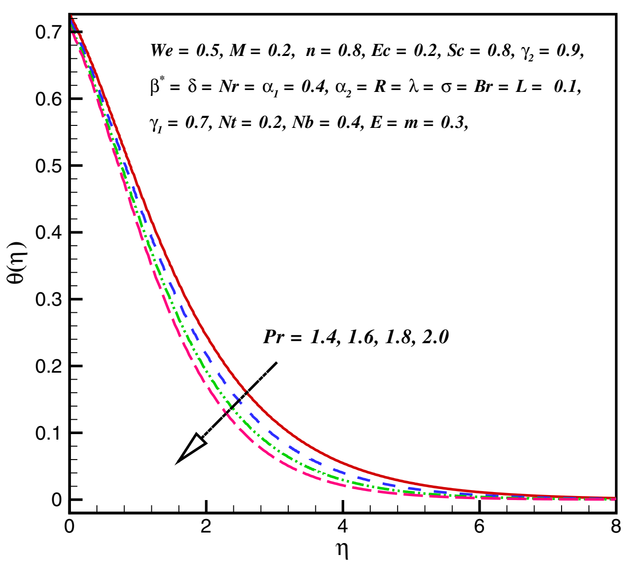

Fig. 7 $\theta(\eta)$ via Pr

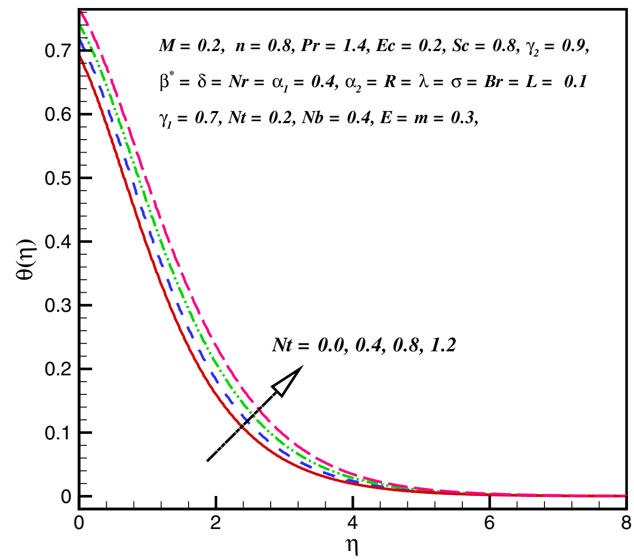

Fig. 8 $\theta(\eta)$ via Nt

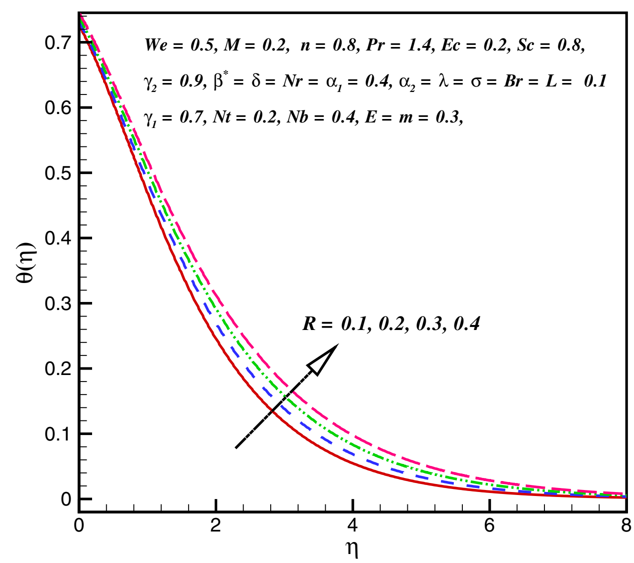

Fig. 9 $\theta(\eta)$ via R

number and heat/mass transfer rate. System of nonhomogeneous ODEs Eq. (8)–(10), (23) and (26) subjected to conditions given in Eq. (11)–(13) is solved by using MATLAB tool bvp4c.

Figure 1 captures influence of We on $f'(\eta)$. Here, we noticed that for larger values of We the $f'(\eta)$ is decreased. Figure 2 depicts outcomes of Nr on velocity profile $(f'(\eta))$. Clearly, $f'(\eta)$ enhances against Nr. Figure 3 disclosed the effect of λ on velocity profile $(f'(\eta))$. Here, one can note that $f'(\eta)$ is raised against λ. In fact, buoyancy forces rise for larger λ due to which velocity of cross-liquid intensifies. Variation of velocity profile $(f'(\eta))$ through magnetic parameter M is examined in Fig. 4. Obviously, $f'(\eta)$ decreased by M. Lorentz force has direct relation with magnetic parameter M. Thus, for higher values of M, the Lorentz force enhances and consequently more resistance decays the fluid motion. Figure 5 shows aspects of β^* on $f'(\eta)$. For higher estimation of β^*, the velocity of cross-nanofluid intensifies.

Behaviors of Ec (Eckert number), Pr (Prandtl number), Nt (thermophoresis parameter) R (radiation parameter) and β^* (ratio of the infinite shear rate viscosity to the zero shear rate viscosity) on $\theta(\eta)$ are sketched in Figs. 6, 7, 8, 9 and 10.

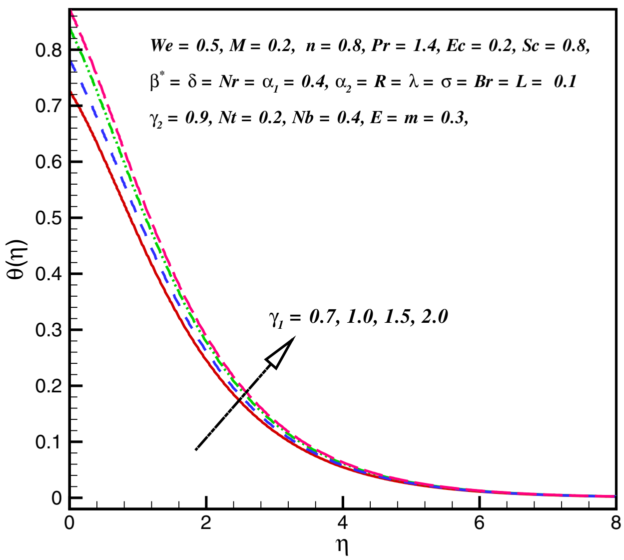

Fig. 10 $\theta(\eta)$ via γ_1

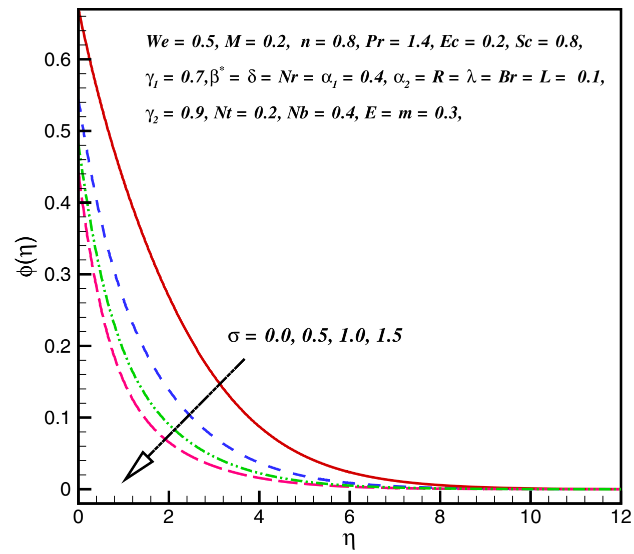

Fig. 12 $\phi(\eta)$ via σ

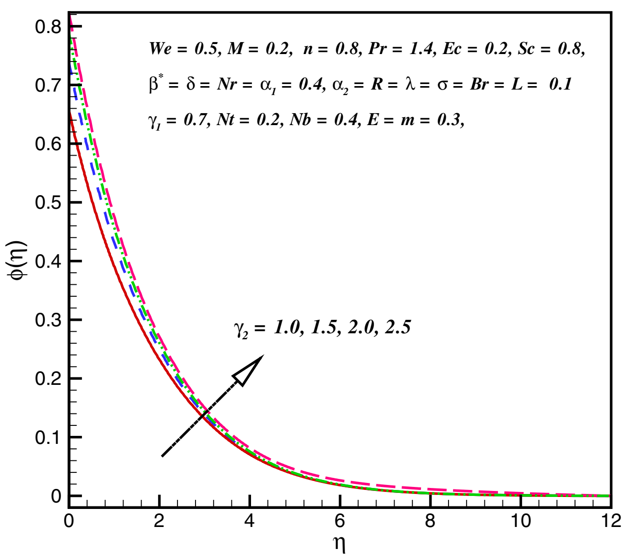

Fig. 11 $\phi(\eta)$ via γ_2

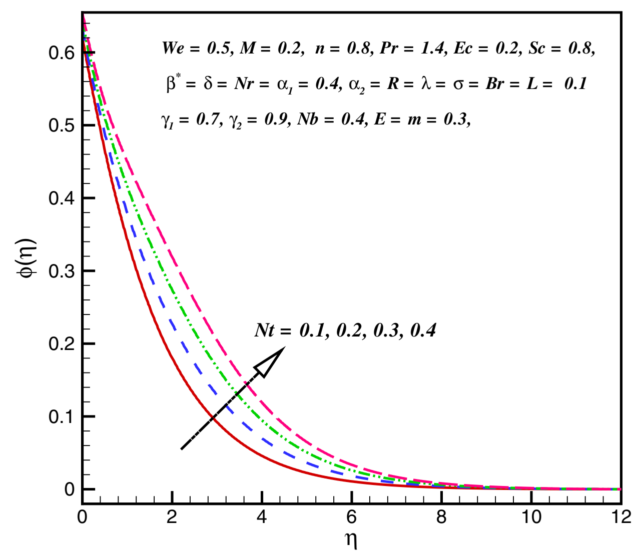

Fig. 13 $\phi(\eta)$ via Nt

Figure 6 addresses the Ec impact on $\theta(\eta)$. Clearly, cross-nanoliquid thermal field remarkably enhances via Ec. In fact, Ec is the ratio between KE (kinetic energy) and enthalpy difference. Consequently, larger Ec generates more resistance in liquid motion and therefore $\theta(\eta)$ intensifies. Figure 7 shows the behaviors of Pr on $\theta(\eta)$. It is perceived that $\theta(\eta)$ declined for lager Pr. Physically, thermal diffusivity deteriorates for large Pr and consequently, $\theta(\eta)$ decreases. Aspects of Nt on $\theta(\eta)$ are shown in Fig. 8. An increase in Nt leads to an enhancement in $\theta(\eta)$. Physically, reason behind this trend of Nt is the gap between reference and surface temperature. For larger Nt, this gap rises and consequently the kinetic energy of nanoparticles enhances. So, $\theta(\eta)$ intensifies. $\theta(\eta)$ is raised against R. These features are reported in Fig. 9. Effect of γ_1 on $\theta(\eta)$ is depicted in Fig. 10. It can be seen from Fig. 10 that $\theta(\eta)$ intensifies via γ_1. Physical reason behind this trend of γ is that less resistance is faced by the thermal wall which causes an enhancement in convective heat transfer to the fluid.

Rheological properties of Sc (Schmidt number), γ_2 (concentration Biot number), σ (dimensionless reaction rate), N_t (thermophoresis parameter), N_b (Brownian motion parameter) on concentration $\phi(\eta)$ are explored in Figs. 11, 12, 13, 14 and 15. Figure 11 captures influence of γ_2 on $\phi(\eta)$. Here,

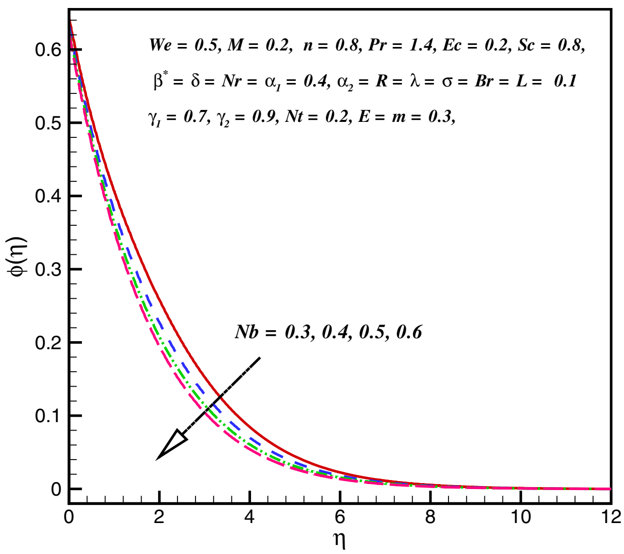

Fig. 14 $\phi(\eta)$ via N_b

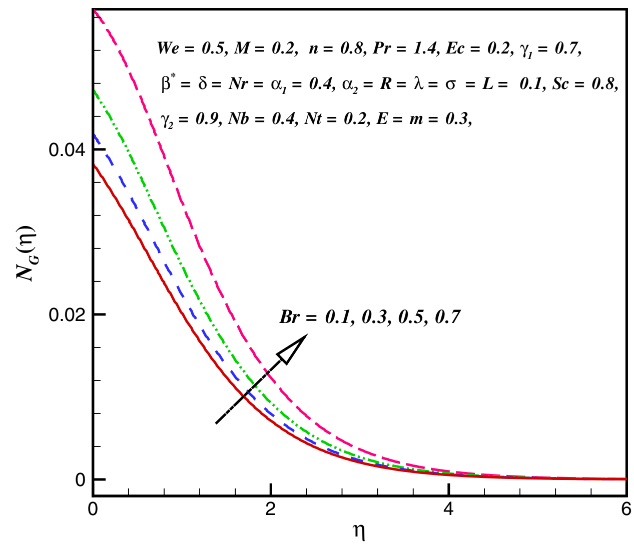

Fig. 16 $N_G(\eta)$ via Br

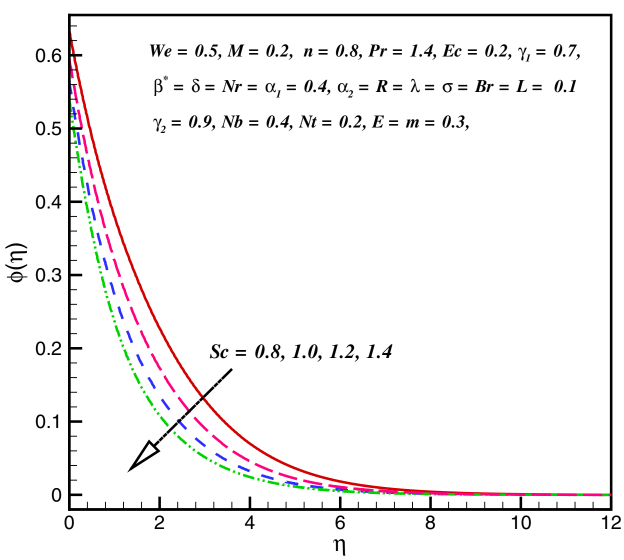

Fig. 15 $\phi(\eta)$ via Sc

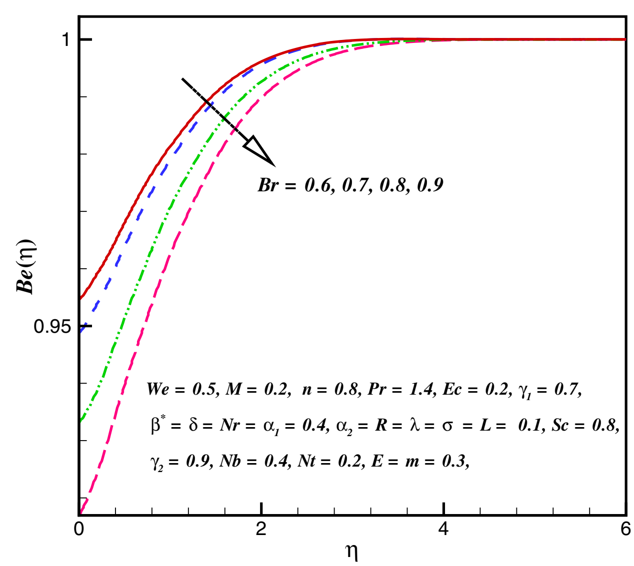

Fig. 17 $Be(\eta)$ via Br

we noted that for larger values of γ_2 the $\phi(\eta)$ is augmented. Figure 12 describes the influence of σ on $\phi(\eta)$. Concentration $\phi(\eta)$ deteriorates via σ. Figures 13 and 14 demonstrate the behavior of N_t and N_b on concentration $\phi(\eta)$. Concentration of cross-nanoliquid $\phi(\eta)$ is enhanced with larger N_t, while $\phi(\eta)$ declines for greater N_b. In fact, when we rise N_t gap of temperature between surface and at infinity intensifies due to which nanofluid moves from higher temperature to lower temperature. Consequently, $\phi(\eta)$ intensifies. Effects of Sc on $\phi(\eta)$ are reported in Fig. 15. Clearly, $\phi(\eta)$ deteriorates via larger Sc.

Variations of N_G (entropy generation) and Bejan number (Be) through Br (Brinkman number), L (diffusive variable), M (magnetic parameter), α_1 (dimensionless concentration ratio variable), α_2(dimensionless temperature ratio variable) and R (thermal radiation parameter) are presented through Figs. 16, 17, 18, 19, 20, 21, 22, 23, 24. Figures 16 and 17 examined the characteristics of Br on N_G and Be. Clearly, N_G are boosted via larger Be, while Be declines for greater Be. Physically, greater Br provides low thermal conduction to nanofluid and consequently, N_G intensifies for larger Br. Outcomes of L (diffusive variable) on N_G are disclosed in Fig. 18. N_G declines for higher values of L. Figures 19 and 20 depict outcomes of M (magnetic parameter) on N_G (entropy generation) and Be (Bejan number).

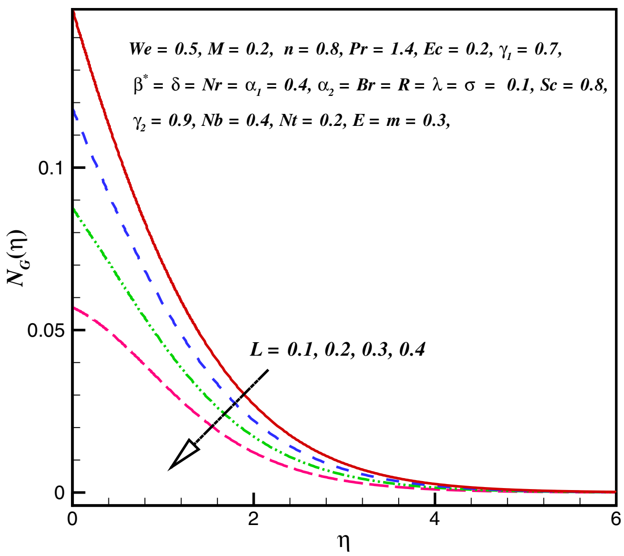

Fig. 18 $N_{\mathrm{G}}(\eta)$ via L

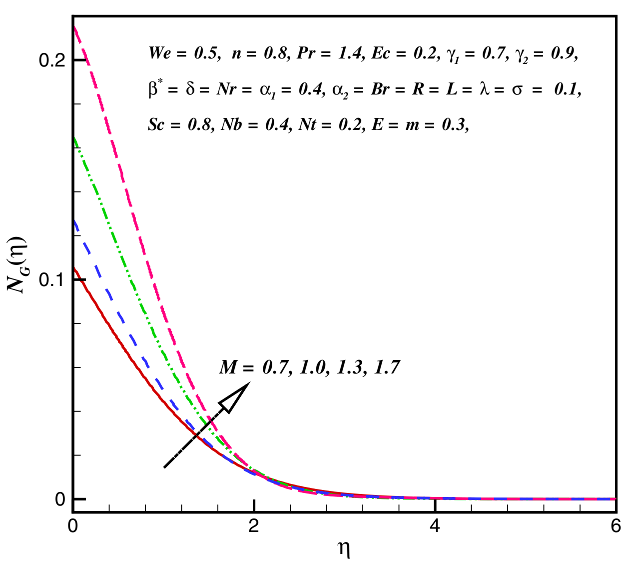

Fig. 19 $N_{\mathrm{G}}(\eta)$ via M

Clearly, N_{G} boosts against M, while Be deteriorates for M. Greater estimation of M (magnetic parameter) offers more resistance to the motion of fluid in system and therefore, heat in the system intensifies. Consequently, entropy rate rises. Impact of α_1 (dimensionless concentration ratio variable) and α_2(dimensionless temperature ratio variable) on entropy rate N_{G} is presented in Figs. 21 and 22. Here, N_{G} is an increasing function of α_1 and α_2. Figures 23 and 24 report the impact of R (thermal radiation parameter) on N_{G} and Be. Clearly, N_{G} shows rising trend for R, while opposite trend is detected for Be. In fact, rise in R produces greater inertial force, so viscous force deteriorates and therefore the entropy rate intensifies.

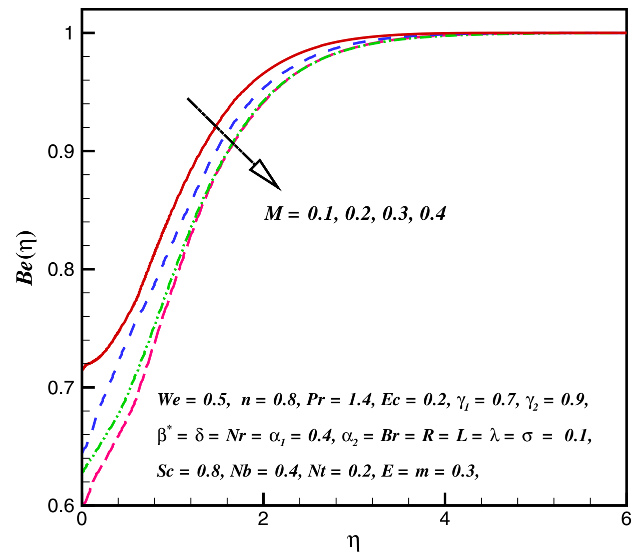

Fig. 20 $Be(\eta)$ via M

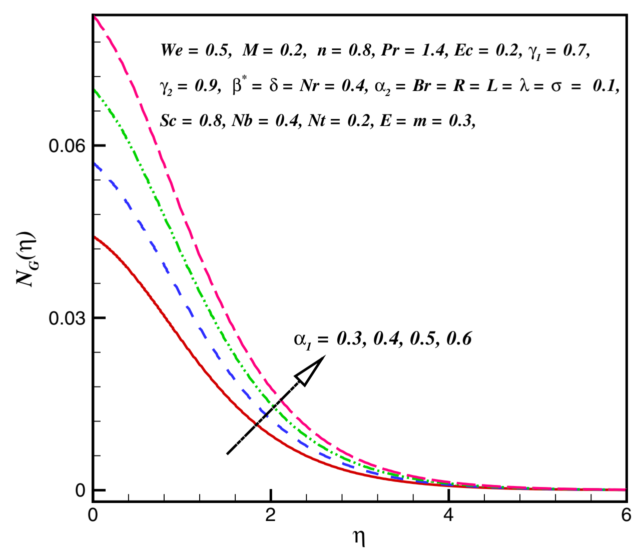

Fig. 21 $N_{\mathrm{G}}(\eta)$ via α_1

Features for n (Power law index), M (magnetic parameter), Ec (Eckert number), Pr(Prandtl number), N_r (buoyancy ratio parameter), N_{t} (thermophoresis parameter) R (radiation parameter) and β^* (ratio of the infinite shear rate viscosity to the zero shear rate viscosity) on skin friction $\left(Re^{1/2}C_{fx}\right)$ Nusselt and number $\left(Nu_x Re_x^{-1/2}\right)$ are computed in Tables 1 and 2. Here, we observed that surface drag force boosts via larger We and M, whereas it declines for larger λ, n and β^*. Table 2 is prepared to point out aspects of numerous physical parameters on $\left(Nu_x Re_x^{-1/2}\right)$. It is scrutinized that transportation rate of heat intensifies via larger Pr, whereas it decays for larger Ec,N_{t} and N_{b}.

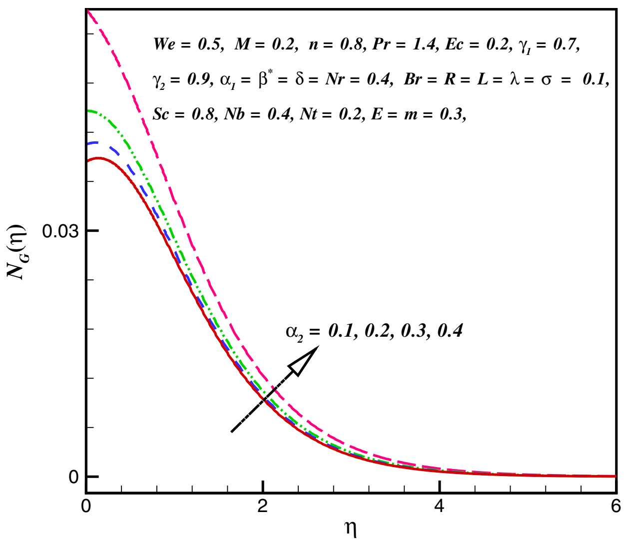

Fig. 22 $N_G(\eta)$ via α_2

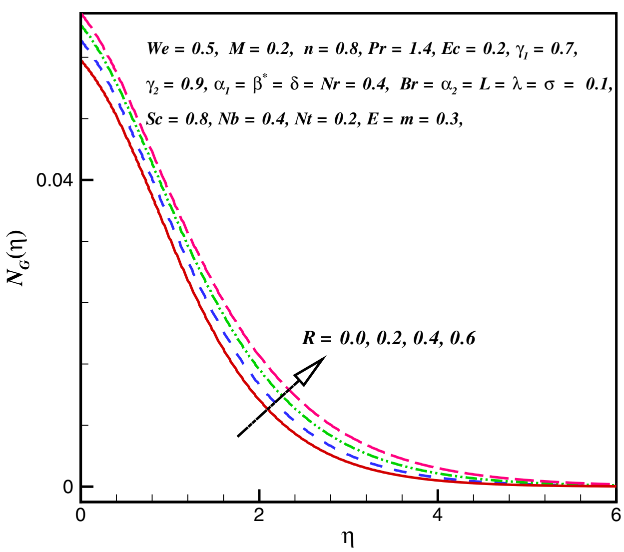

Fig. 23 $N_G(\eta)$ via R

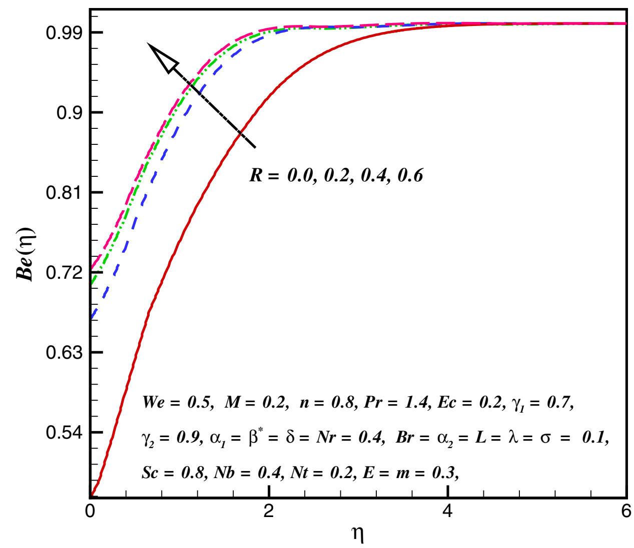

Fig. 24 $Be(\eta)$ via R

6 Concluding remarks

We have the following significant observations.

- Lorentz's force for cross-nanoliquid is used as resistive force which controls the liquid motion.
- Velocity is increasing function of β^*.
- Temperature $\theta(\eta)$ intensifies via N_t and N_b, while it is reduced with Pr.
- Enhancement in $\phi(\eta)$ (Concentration) occurs for augmented values of E (activation energy).
- N_G (rate of entropy generation) boosts for larger Br (Brinkman number), M (magnetic parameter), α_1 (dimensionless concentration ratio variable), α_2(dimensionless temperature ratio variable) and R (thermal radiation parameter); however, it decayed via larger L (diffusive variable).
- Bejan number (Be) rises for greater estimation of R (thermal radiation parameter), while it deteriorates for Br (Brinkman number).

Table 1 Surface drag force $\left(Re^{1/2}C_{fx}\right)$ via different estimation of physical parameters

We	n	λ	β^*	M	Nr	$-Re^{\frac{1}{2}}C_{fx}$
0.5	0.1	0.1	0.4	0.1	0.2	1.018466
0.8						1.9379354
1.0						1.8971728
1.2	0.2					0.8544199
	0.5					0.7075146
	0.8					0.5757617
		0.2				0.8001096
		0.3				0.6210907
		0.5				0.5359078
			0.6			0.9033084
			0.8			0.8808326
			1.0			0.8649508
				0.3		0.7913559
				0.5		0.8234892
				0.7		0.8827631
					0.3	0.858133
					0.4	0.8596886
					0.5	0.8822489

Table 2 Computational outcomes for rate of heat transfer $(Re^{-1/2}Nu)$

β^*	Pr	Ec	Nt	Nb	R	$Nu_xRe^{-\frac{1}{2}}$
0.0	0.2	0.1	0.2	0.4	0.5	0.202193
0.1						0.18603
0.2						0.178439
0.4	0.5					0.228093
	0.7					0.25841
	0.9					0.284055
		0.3				0.163207
		0.7				0.147585
		0.9				0.108134
			0.5			0.169995
			0.8			0.169995
			1.0			0.168315
				0.5		0.170431
				0.6		0.169881
				0.7		0.169451
					0.8	0.20144
					1.0	0.181581
					1.2	0.175118

Acknowledgements This project was funded by the postdoctoral international exchange program for incoming postdoctoral students, at Beijing Institute of Technology, Beijing, China.

References

1. Khan WA, Khan M (2014) Three-dimensional flow of an Oldroyd-B nanofluid towards stretching surface with heat generation/absorption. PLoS ONE 9(8):e10510
2. Sheikholeslami M, Bandpy MG, Ellahi R, Zeeshan A (2014) Simulation of MHD CuO-water nanofluid flow and convective heat transfer considering Lorentz forces. J Magn Mag Mat 369:69–80

3. Khan M, Khan WA (2015) Forced convection analysis for generalized Burgers nanofluid flow over a stretching sheet. AIP Adv 5:107138. https://doi.org/10.1063/1.4935043
4. Khan M, Khan WA (2016) MHD boundary layer flow of a power-law nanofluid with new mass flux condition. AIP Adv 6:025211. https://doi.org/10.1063/1.4942201
5. Waqas M, Farooq M, Khan MI, Alsaedi A, Hayat T, Yasmeen T (2016) Magnetohydrodynamic (MHD) mixed convection flow of micropolar liquid due to nonlinear stretched sheet with convective condition. Int J Heat Mass Transfer 102:766–772
6. Khan M, Khan WA, Alshomrani AS (2016) Non-linear radiative flow of three-dimensional Burgers nanofluid with new mass flux effect. Int J Heat Mass Transfer 101:570–576
7. Khan M, Khan WA (2016) Steady flow of Burgers nanofluid over a stretching surface with heat generation/absorption. J Braz Soc Mech Sci Eng 38(8):2359–2367
8. Hayat T, Rashid M, Imtiaz M, Alsaedi A (2017) MHD effects on a thermo-solutal stratified nanofluid flow on an exponentially radiating stretching sheet. J Appl Mech Tech Phys. https://doi.org/10.1134/s0021894417020043
9. Ahmad L, Khan M, Khan WA (2017) Numerical investigation of magneto-nanoparticles for unsteady 3D generalized Newtonian liquid flow. Eur Phys J Plus 132:373. https://doi.org/10.1140/epjp/i2017-11658-6
10. Khan M, Irfan M, Khan WA (2017) Impact of nonlinear thermal radiation and gyrotactic microorganisms on the Magneto-Burgers nanofluid. Int J Mech Sci 130:375–382
11. Waqas M, Ijaz Khan M, Hayat T, Alsaedi A, Imran Khan M (2017) Nonlinear thermal radiation in flow induced by a slendering surface accounting thermophoresis and Brownian diffusion. Eur Phys J Plus 132:280. https://doi.org/10.1140/epjp/i2017-11555-0
12. Khan M, Irfan M, Khan WA (2017) Numerical assessment of solar energy aspects on 3D magneto-Carreau nanofluid: a revised proposed relation. Int J Hydrogen Energy 42(34):22054–22065
13. Waqas M, Khan MI, Hayat T, Alsaedi A (2017) Stratified flow of an Oldroyd-B nanoliquid with heat generation. Results Phys 7:2489–2496
14. Sohail A, Shah SIA, Khan WA, Khan M (2017) Thermally radiative convective flow of magnetic nanomaterial: a revised model. Results Phys 7:2439–2444
15. Khan WA, Irfan M, Khan M, Alshomrani AS, Alzahrani AK, Alghamdi MS (2017) Impact of chemical processes on magneto nanoparticle for the generalized Burgers fluid. J Mol Liq 234:201–208
16. Animasaun IL, Mahanthesh B, Jagun AO, Bankole TD, Sivaraj R, Shah NA, Saleem S (2018) Significance of Lorentz force and thermoelectric on the flow of 29 nm CuO-Water nanofluid on an upper horizontal surface of a paraboloid of revolution. J Heat Transfer 141(2):022402
17. Sheikholeslami M, Seyednezhad M (2018) Simulation of nanofluid flow and natural convection in a porous media under the influence of electric field using CVFEM. Int J Heat Mass Transfer 120:772–781
18. Waqas M, Hayat T, Alsaedi A (2018) A theoretical analysis of SWCNT–MWCNT and H2O nanofluids considering Darcy-Forchheimer relation. Appl Nanosci. https://doi.org/10.1007/s13204-018-0833-6
19. Muhammad T, Dian-Chen Lu, Mahanthesh B, Eid Mohamed R, Ramzan M, Dar A (2018) Significance of Darcy-Forchheimer porous medium in nanofluid through carbon nanotubes. Commun Theor Phys 70(3):361
20. Irfan M, Khan M, Khan WA, Ayaz M (2018) Modern development on the features of magnetic field and heat sink/source in Maxwell nanofluid subject to convective heat transport. Phys Lett A 382(30):1992–2002
21. Sheikholeslami M, Jafaryar M, Shafee A, Li Z (2018) Investigation of second law and hydrothermal behavior of nanofluid through a tube using passive methods. J Mol Liq 269:407–416
22. Khan WA, Alshomrani AS, Alzahrani AK, Khan M, Irfan M (2018) Impact of autocatalysis chemical reaction on nonlinear radiative heat transfer of unsteady three-dimensional Eyring-Powell magneto-nanofluid flow. Pramana-J Phys 91:63. https://doi.org/10.1007/s12043-018-1634-x
23. Gireesha BJ, Mahanthesh B, Thammanna GT, Sampathkumar PB (2018) Hall effects on dusty nanofluid two-phase transient flow past a stretching sheet using KVL model. J Mol Liq 256:139–147
24. Amala S, Mahanthesh B (2018) Hybrid nanofluid flow over a vertical rotating plate in the presence of hall current, Nonlinear convection and heat Absorption. J Nanofluids 7(6):1138–1148
25. Sheikholeslami M, Shehzad SA (2018) Simulation of water based nanofluid convective flow inside a porous enclosure via non-equilibrium model. Int J Heat Mass Transfer 120:1200–1212
26. Alshomrani AS, Zaka Ullah M, Capizzano SS, Khan WA, Khan M (2019) Interpretation of chemical reactions and activation energy for unsteady 3D flow of Eyring-Powell magneto-nanofluid. Arab J Sci Eng 44(1):579–589
27. Sheikholeslami M, Jafaryar M, Shafee A, Li Z, Haq Rizwan-ul (2019) Heat transfer of nanoparticles employing innovative turbulator considering entropy generation. Int J Heat Mass Transfer 136:1233–1240
28. Shruthy M, Mahanthesh B (2019) Rayleigh-bénard convection in Casson and hybrid nanofluids: an analytical investigation. J Nanofluids 8(1):222–229
29. Sheikholeslami M, Rizwan-ulHaq A, Shafee Z, Lie YG Elaraki, Tlili I (2019) Heat transfer simulation of heat storage unit with nanoparticles and fins through a heat exchanger. Int J Heat Mass Transfer 135:470–478
30. Gireesha BJ, Archana M, Mahanthesh B, Prasannakumara BC (2019) Exploration of activation energy and binary chemical reaction effects on nano Casson fluid flow with thermal and exponential space-based heat source. Mult Mod Mater Struct 15(1):227–245
31. Sheikholeslami M, Haq RU, Shafee A, Li Z (2019) Heat transfer behavior of nanoparticle enhanced PCM solidification through an enclosure with V shaped fins. Int. J Heat Mass Transfer 130:1322–1342
32. Khan M, Irfan M, Khan WA, Sajid M (2019) Consequence of convective conditions for flow of Oldroyd-B nanofluid by a stretching cylinder. J Braz Soc Mech Sci Eng 41:116. https://doi.org/10.1007/s40430-019-1604-3
33. Animasaun IL, Koriko OK, Adegbie KS, Babatunde HA, Ibraheem RO, Sandeep N, Mahanthesh B (2019) Comparative analysis between 36 nm and 47 nm alumina-water nanofluid flows in the presence of Hall effect. J Therm Anal Calorim 135(2):873–886
34. Sheikholeslami M (2019) New computational approach for exergy and entropy analysis of nanofluid under the impact of Lorentz force through a porous media. Comput Methods Appl Mech Eng 344:319–333
35. Abbas SZ, Khan WA, Sun H, Ali M, Irfan M, Shahzed M, Sultan F (2019) Mathematical modeling and analysis of Cross nanofluid flow subjected to entropy generation. Appl Nanosci. https://doi.org/10.1007/s13204-019-01039-9
36. Sheikholeslami M (2019) Numerical approach for MHD Al2O3-water nanofluid transportation inside a permeable medium using innovative computer method. Comput Methods Appl Mech Eng 344:306–318
37. Ali M, Khan WA, Irfan M, Sultan F, Shahzed M, Khan M (2019) Computational analysis of entropy generation for

cross-nanofluid flow. Appl Nanosci. https://doi.org/10.1007/s13204-019-01038-w

38. Sheikholeslami M, Gerdroodbary MB, Moradi R, Shafee A, Li Z (2019) Application of Neural Network for estimation of heat transfer treatment of Al2O3-H2O nanofluid through a channel. Comput Methods Appl Mech Eng 344:1–12
39. Sultan F, Khan WA, Ali M, Shahzad M, Irfan M, Khan M (2019) Theoretical aspects of thermophoresis and Brownian motion for three-dimensional flow of the cross fluid with activation energy. Pramana-J Phys 92:21. https://doi.org/10.1007/s12043-018-1676-0
40. Sheikholeslami M, Mahian Omid (2019) Enhancement of PCM solidification using inorganic nanoparticles and an external magnetic field with application in energy storage systems. J Clean Prod 215:963–977
41. Khan M, Irfan M, Khan WA (2019) Heat transfer enhancement for Maxwell nanofluid flow subject to convective heat transport. Pramana-J Phys. https://doi.org/10.1007/s12043-018-1690-2
42. Nematpour Keshteli A, Sheikholeslami M (2019) Nanoparticle enhanced PCM applications for intensification of thermal performance in building: a review. J Mol Liq 274:516–533
43. Khan WA, Alshomrani AS, Khan M (2016) Assessment on characteristics of heterogeneous-homogenous processes in three-dimensional flow of Burgers fluid. Results Phys 6:772–779
44. Khan WA, Khan M, Alshomrani AS (2016) Impact of chemical processes on 3D Burgers fluid utilizing Cattaneo-Christov double-diffusion: applications of non-Fourier's heat and non-Fick's mass flux models. J Mol Liq 223:1039–1047
45. Mahanthesh B, Gireesha BJ, Athira PR (2017) Radiated flow of chemically reacting nanoliquid with an induced magnetic field across a permeable vertical plate. Results Phys 7:2375–2383
46. Sohail A, Khan WA, Khan M, Shah SIA (2017) Consequences of non-Fourier's heat conduction relation and chemical processes for viscoelastic liquid. Results Phys 7:3281–3286
47. Hayat T, Khan MI, Waqas M, Alsaedi A, Yasmeen T (2017) Diffusion of chemically reactive species in third grade fluid flow over an exponentially stretching sheet considering magnetic field effects. Chin J Chem Eng 25(3):257–263
48. Irfan M, Khan M, Khan WA (2018) Interaction between chemical species and generalized Fourier's law on 3D flow of Carreau fluid with variable thermal conductivity and heat sink/source: a numerical approach. Results Phys 10:107–117
49. Khan MI, Qayyum S, Hayat T, Khan MI, Alsaedi A, Khan TA (2018) Entropy generation in radiative motion of tangent hyperbolic nanofluid in presence of activation energy and nonlinear mixed convection. Phys Lett A 382:2017–2026
50. Khan WA, Sultan F, Ali M, Shahzad M, Khan M, Irfan M (2019) Consequences of activation energy and binary chemical reaction for 3D flow of Cross-nanofluid with radiative heat transfer. J Braz Soc Mech Sci Eng 41:4. https://doi.org/10.1007/s40430-018-1482-0
51. Waqas M, Naz S, Hayat T, Alsaedi A (2019) Numerical simulation for activation energy impact in Darcy-Forchheimer nanofluid flow by impermeable cylinder with thermal radiation. Appl Nanosci 15:17. https://doi.org/10.1007/s13204-018-00940-z
52. Khan WA, Ali M, Sultan F, Shahzad M, Khan M, Irfan M (2019) Numerical interpretation of autocatalysis chemical reaction for nonlinear radiative 3D flow of cross magnetofluid. Pramana-J Phys 92:16. https://doi.org/10.1007/s12043-018-1678-y